Some physical properties of the ZnO films obtained by electrodeposition using Zn (NO₃) .6H₂O aqueous solution at different cathodic potentials

Ayça Kıyak Yıldırım [1*], Barış Altıokka [2]

ABSTRACT

Polycrystalline ZnO films prepared by electrodeposited on ITO coated glass substrate at different cathodic potential were investigated. In all experiments Zn(NO3).6H₂O aqueous solution was used as an electrolyte and depositions temperature were kept at 72°C for the period of the depositions. Cyclic voltammetry experiments were performed to determinate the cathodic potential ranging for electrodeposition. After that, the cathodic potential ranging from -0.8 to -1.16 V were selected. Characterization of polycrystalline ZnO films was realized using X-ray diffraction (XRD), UV-vis spectrophotometer and scanning electron microscopy (SEM) methods .XRD results shown that all films formed in hexagonal crystal structure and crystallite sizes of the all films are approximately 46 nm. The energy band gaps of the ZnO films are from 3.50 to 3.56 eV. It was understood from the SEM images that the morphology of polycrystalline ZnO films depends greatly on the cathodic potential of depositions. Also various morphological structure was found such as slicely, lamellar and lace like structure.

Keywords: ZnO, Cathodic potential, Energy Band Gap

Farklı katodik potansiyellerde Zn (NO₃) .6H₂O sulu çözeltisi kullanılarak elektrodepozisyon yöntemi ile elde edilen ZnO filmlerin bazı fiziksel özellikleri

ÖZ

Farklı katodik potansiyellerde ITO kaplı cam alt tabaka üzerinde elektrokimyasal depozisyon ile hazırlanan polikristal ZnO filmler incelenmiştir. Tüm deneylerde, Zn (NO₃) .6H₂O sulu çözeltisi elektrolit olarak kullanılmıştır ve depozisyon sıcaklığı depozisyon boyunca 72°C tutulmuştur. Dönüşümlü voltametri deneyleri elektrodepozisyon için katodik potansiyel aralığının tespiti için yapılmıştır. Bundan sonra, -0.80 V'den 1,16 V'ye kadar artarak değişen katodik potansiyel aralığı seçilmiştir. Polikristal ZnO filmlerin karakterizasyonu X-ışını kırınımı (XRD), UV-vis spektrofotometre ve taramalı elektron mikroskobu (SEM) yöntemleri kullanılarak gerçekleştirilmiştir. XRD sonuçları, tüm filmlerin altıgen kristal yapısında olduğunu ve tüm filmlerin yaklaşık olarak 46 nm tane büyüklüğünde oluşturulmuş olduğunu göstermiştir. ZnO filmlerin enerji bant aralığı 3.50 eV' ile 3.56 eV aralığında değişmektedir. Polikristalin ZnO filmlerin morfolojisi büyük ölçüde elektrokimyasal depozisyon işleminin katodik potansiyeline bağlı olduğu SEM görüntülerinden anlaşılmaktadır. Ayrıca dilim şeklide, pullu ve dantele benzeyen çeşitli morfolojik yapılar bulunmuştur.

Anahtar Kelimeler: ZnO, katodik potansiyel , Enerji band aralığı

* Sorumlu Yazar / Ayça Kıyak Yıldırım
[1*] Ayça Kıyak Yıldırım, Bilecik Şeyh Edebali Üniversitesi, Meslek Yüksek Okulu, Motorlu Araçlar ve Ulaştırma Teknolojisi Bölümü Otomotiv Teknolojisi Programı, Bilecik-ayca.kiyak@bilecik.edu.tr
[2] Barış Altıokka, Bilecik Şeyh Edebali Üniversitesi, Meslek Yüksek Okulu, Elektrik ve Enerji Bölümü Elektrik Enerjisi Üretim, İletim ve Dağıtımı Programı, Bilecik-baris.altiokka@bilecik.edu.tr

1. INTRODUCTION

Zinc oxide (ZnO) is a non-toxic and has wide bandgap semiconductor which is $Eg = 3.20$ eV also it has natural n-type electrical conductivity [1]. ZnO films have been growth vary different techniques like RF magnetron sputtering, molecular beam epitaxy, metal organic chemical vapour deposition, pulsed laser deposition and spray pyrolysis, sol-gel [2]. plasma-assisted molecular beam epitaxy and electrodeposition [3]. Zinc oxide is one of the most encouraging materials for nanotechnology owing to its range of prospective applications such as sensors, photovoltaic cells, light-emitting diodes and nanogenerators [4]. As another synthesis methods, electrochemical deposition represents the advantage of having low temperature processing, allows various substrate shapes and controllable film thickness. [1]. The mechanisms of oxide deposition with ZnO film committed by Izaki are revealed by following reactions equations [5].

$$Zn(NO_2)_2 \rightarrow Zn^{2+} + 2NO_3^- \qquad (1)$$
$$NO_3^- + H_2O + 2e^- \rightarrow NO_2 + 2OH^- \qquad (2)$$
$$Zn^{2+} + 2OH^- \rightarrow Zn(OH)_2 \qquad (3)$$
$$Zn(OH)_2 \rightarrow ZnO + H_2O \qquad (4)$$

Conductive materials such as indium tin oxide (ITO) must be used for occurring these reactions. In consequence of that the conductive materials have to be very clean. If conductive material is dirty, these reactions will not come off.

2. MATERIAL AND METHOD

In this study, polycrystalline ZnO films were produced by electrodeposition from aqueous solutions composed of 0.01 M Zn(NO3)$_2$.6H$_2$O. The pH value of aqueous solution was measured by a pH meter and it was adjusted to be 6.22. The final solutions were kept at constant value of $70\pm2°C$ temperature during the deposition. Throughout the depositions aqueous solutions were bubling with oxygen by passing oxygen through the growth cell. IVIUM VERTEX Potentiostat/Galvanostat system with conventional three electrode cell with counter electrode, a platinum wire and a saturated calomel reference electrode was used for electrodeposition. ITO coated glass substrates having sheet resistance of 25 Ω/cm with an effective deposition area of 1.65 cm^2 were used as the working electrode for the electrodeposition of ZnO films. Prior to thedeposition, ITO coated glass substrates were washed thoroughly with acetone and subsequently deionized water then being cleaned ultrasonically after that they were given up for drying under ambient condition. An Ag/AgCl saturated electrode was employed like as the reference electrode, a platinum wire the counter electrode to electrodeposition of ZnO thin films. Electrodepositions were exerted potentiostatically with stirring 600 rpm at different cathodic potentials between -0.80 V and 1.16 V (versus Ag/AgCl) for 30 minute of deposition time. The optical properties of the films were ascertained with using absorbance measurements which were acquired by UV-vis spectrophotometer at wavelength 300nm and 600nm. The structural analyses of the films were realized by using XRD. The morphological properties of the films were examined by a SEM.

3. CONCLUSIONS AND DISCUSSION

3.1. XRD Analysis of the ZnO Films

The current density curves during the electrodeposition process are demonstrate in Figure. 1 .Whole these curves were used to calculate of film thicknesses. These films thickness can be account using the Faraday's law which is dedicated the following formula:

$$t = \frac{1}{n.F.A}\left(\frac{Q.M}{\rho}\right) \qquad (5)$$

where F is Faraday's number, n is the number of electrons transferred, Q is the charge pending the electrodeposition process, A is the area of the electrode, M is 81.4 g/mol and ρ is the density (5.6 g/cm3) [6]. Actually, these thicknesses are the some rough values due to the current efficiency during the electrodeposition process is reputed to be 100%. Because of the touch the film thicknesses additionally were calculated gravimetric method. The calculated film thicknesses are given in Table 1. If Table 1 perused, the film thicknesses are increased depend on the increasing cathodic potential excepted thicknesses of the film obtained in -0.90 V cathodic potential.

Table 1 The thicknesses, crystallite sizes and band gap of the ZnO films

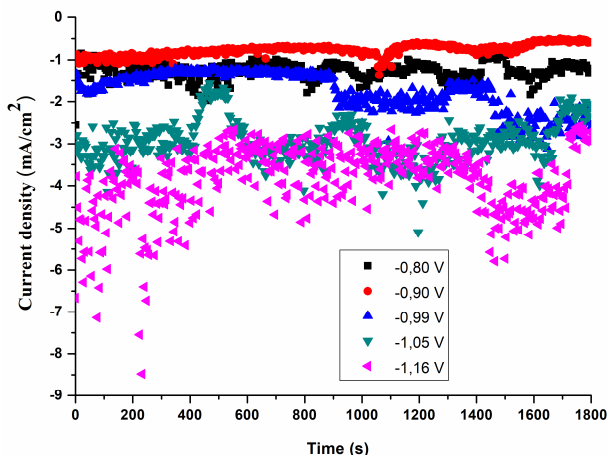| Experiment	-0.80V	-0.90V	-0.99V	-1.05V	-1.16V
Thicknes(nm)	1727	1067	2438	4054	**5322**
Crystallite size (nm)	45	46	44	47	**48**
Bandgap (eV)	**3.56**	**3.53**	**3.56**	**3.51**	**3.50**

Figure 1. The current density versus time of ZnO films

Figure. 2 shows the X-ray diffraction patterns of ZnO films. It indicate seven peaks and these peaks are due to the diffraction of (010), (002), (011), (012), (110), (013) and (112) planes. All the diffraction compatible to ASTM card which is the hexagonal structure of ZnO and is indexed number of (98-006-5122). Also, the films which are obtained in -0.90 V and -0.99

V cathodic potentials have the diffraction of (010) planes which compatible to ASTM card is indexed number of (98-016-3380) are to identified. Additionally, the film which is produced by 1,16 V cathodic potentials has the diffraction of (010) planes which well-match ASTM card is indexed number of (98-016-3380) is to be determinate.

The peak intensities of the films acquired in 1.16 V and -1.05 V cathodic potentials are very higher than that of the other films. The results of XRD pattern shows the films which are obtained in all cathodic potentials have only one intense diffraction peak that indwell at average 34° demonstrating that (002) is the preferential crystal orientation.

On account of apprising the preferred orientation of ZnO films the texture coefficient (TC) is utilized and calculated the following equation.

$$TC(hkl) = \frac{\frac{I(hkl)}{I_0(hkl)}}{(\frac{1}{N})\left[\Sigma_N \frac{I(hkl)}{I_0(hkl)}\right]} \qquad (6)$$

where TC(hkl) is the texture coefficient of the (hkl) plane, I is the measured intensity, I_0 is standard intensity JCPDS and N is the number of diffraction peaks [7]. The calculated texture coefficient of the films, peak angles of the films and intensity of the films which is related to the diffraction of plane obtained in all films were given in Table 2 and the TC of the films demonstrate that preferred orientation of the all films is (002) plane except the film which is produced by 1,16 V cathodic potential.
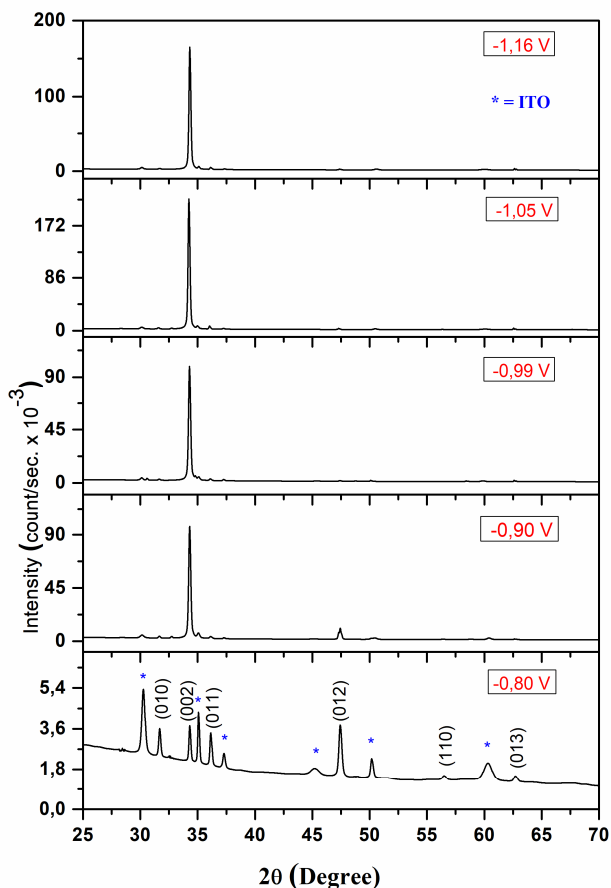

Figure 2. X-ray diffraction patterns of the ZnO films

The average crystallite sizes of the ZnO films were interpreted from using the full width at half maximum (FWHM), corrected by the XRD line broadening applying the Scherrer method that is revealed by the following equation.

$$cs = \frac{K \times \lambda}{\beta \times cos\theta} \qquad (7)$$

where 2θ is the position of peak center, λ is the wavelength of X-ray radiation (1.54056 Å), β is the full width at the half maximum of peak height (in degrees) [8]. The crystallite sizes of the film are given in Table 1. As the cathodic potential was increased the crystallite size is nearly same. It was concluded that increasing cathodic potential don't effect crystallite sizes.

Table 2. The calculated texture coefficient, peak angles and intensity of the films

Experiment	2θ	Intensity (counts/sec)	I/I_0	TC	(hkl)
-0.80 v	**31.661**	**3545**	**96.56**	**1.04**	**(010)**
	34.287	**3642**	**99.19**	**1.07**	**(002)**
	36.133	**3406**	**92.76**	**1.00**	**(011)**
	47.391	**3671**	**100**	**1.08**	**(012)**
	56.829	1357	36.97	0.40	(110)
	62.670	1424	38.77	0.42	(013)
Experiment	2θ	Intensity (counts/sec)	I/I_0	TC	(hkl)
-0.90 V	31.635	4188	4.32	0.21	(010)
	32.727	4032	4.16	0.20	(010)
	34.313	**96883**	**100**	**4.78**	**(002)**
	36.133	3930	4.06	0.19	(011)
	47.443	10766	11.11	0.53	(012)
	62.627	1819	1.88	0.09	(013)
Experiment	2θ	Intensity (counts/sec)	I/I_0	TC	(hkl)
-0.99 V	31.635	3103	3.14	0.16	(010)
	32.701	4271	4.32	0.23	(010)
	34.287	**98920**	**100**	**5.22**	**(002)**
	36.107	3390	3.43	0.18	(011)
	47.365	1855	1.88	0.10	(012)
	62.601	2124	2.15	0.11	(013)
Experiment	2θ	Intensity (counts/sec)	I/I_0	TC	(hkl)
-1.05 V	31.557	4730	2.19	0.14	(010)
	34.235	**216051**	**100**	**6.31**	**(002)**
	36.029	7223	3.34	0.21	(011)
	47.261	3528	1.63	0.10	(012)
	56.335	2062	0.95	0.06	(110)
	62.549	4020	1.86	0.12	(013)
	67.645	1991	0.92	0.06	(112)
Experiment	2θ	Intensity (counts/sec)	I/I_0	TC	(hkl)
-1.16 V	31.661	3702	2.25	0.12	(010)
	34.313	**164827**	**100**	**5.45**	**(002)**
	36.133	4935	2.99	0.16	(011)
	47.365	2808	1.70	0.09	(012)
	62.627	3565	2.16	0.12	(013)
	67.671	1685	1.02	0,06	(112)

The residual strains (macro strain) of the acquired film in the c axis were calculated following formula:

$$\varepsilon_{avr} = \frac{\beta}{4\tan\theta} \qquad (9)$$

where ε_{avr} is average strain, β is full width at high maximum and θ is the diffraction angle [9]. The stress (σ) in the ZnO films was revealed using the following equation.

$$\sigma = \frac{2C_{13}^2 - C_{33}(C_{11}+C_{12})}{2C_{13}} \times \varepsilon_{mac} \qquad (10)$$

where C_{11} = 209.7 GPa, C_{12} = 121.1 GPa, C_{13} = 105.1 GPa and C_{33} = 210.9 GPa are the elastic stiffness constants of bulk ZnO [10]. Dislocation density is to be descriptive of the length of dislocation line per unit volume of the crystal. The dislocation density of belonging ZnO films were calculated utilization the following equation.

$$\rho = \frac{\sqrt{1\,2}\langle e^2\rangle^{1/2}}{d \cdot cs} \qquad (11)$$

Where $\langle e^2\rangle^{1/2}$ is the micro strain and d is the interplanar spacing [11]. The micro strains, macro strains, average strains,

stresses and dislocation densities of the all films are demonstrated in Table 3. Meanwhile RMS strain (micro strain) values of the films acquired are between 1.95 and 2.43 which is stand for cathodic potentials reduces micro strain values. The residual strain of the film obtained at -0.80 V cathodic potentials is very high check against with the residual strain of the other films. It is seen that the dislocation density and micro strain of the film obtained at -0.80V are higher than that of the other films. Therefore, it can be say that this film has poor crystallization. The stress of the produced film can be investigated after that investigation it was latch onto the film which is produced by 1.16 V and -0.80 V have highest and lowest stress respectively.

Table 3. The micro strains, macro strains, average strains, stresses and dislocation densities of the ZnO films

Experiment	-0.80 V	-0.90 V	-0.99 V	-1.05 V	-1.16 V
d (Å)	1.920	2.615	2.617	2.620	2.614
a (Å)	3.019	3.266	3.162	3.272	3.264
c (Å)	5.229	5.230	5.233	5.241	5.229
FWHM (°)	0.213	0.207	0.218	0.201	0.197
RMS Strain $\langle e^2\rangle^{1/2}$ $\times 10^{-3}$	2.43	2.34	2.34	1.95	1.95
ResidualStrain Makro Strain $\times 10^{-3}$	18.14	5.95	5.41	6.87	4.59
AverageStrain $\times 10^{-3}$	2.12	2.93	3.08	2.85	2.78
DislocationDensity $\times 10^{+16}$(Line/m^2)	1.98	1.39	1.45	1.24	1.22
Stress GPa	-4.22	-1.39	-1.26	-1.60	-1.07

3.2. Surface Morphologies of the Films

Morphological properties of the films were perused by a SEM with coated platinum. The surfaces were magnified 10000X and 50000X and were given in Fig. 3 together respectively for different cathodical potential.

In the literature ZnO generally form in rods structure. But in this study surfaces weren't covered rods. The surfaces were covered slice like ZnO crystals. Under this slice like structure there are lamellar like structures. It may be important that when surface areas of the films increase, it can be suitable for gas sensors.

Figure 3a. Relatively low (10000X) and high (50000) magnification top-view SEM images of ZnO films obtained in -0.80 V
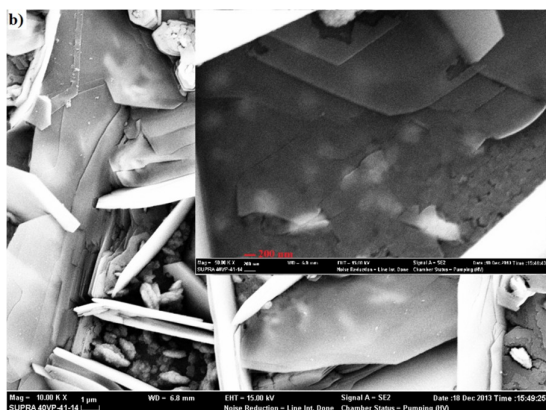

Figure 3d. Relatively low (10000X) and high (50000) magnification top-view SEM images of ZnO films obtained in -1.05 V
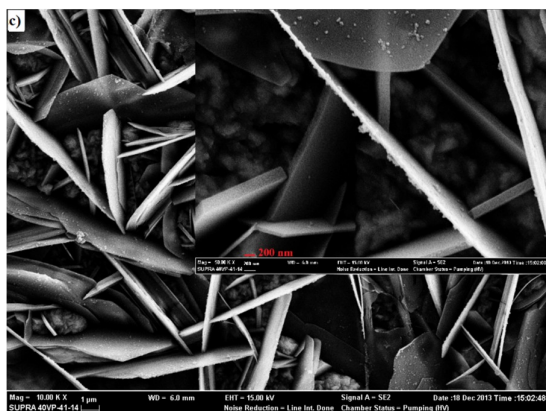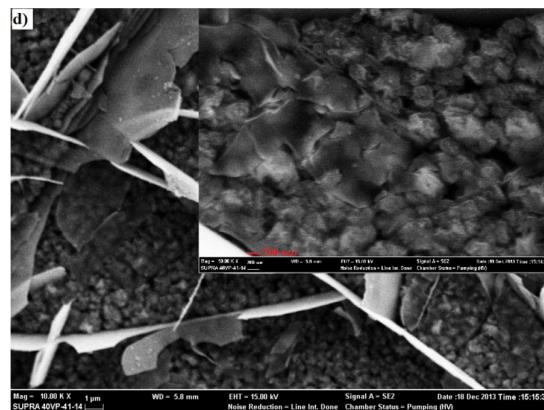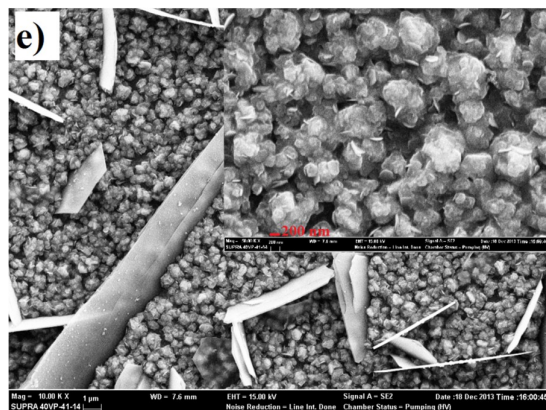

Figure 3b. Relatively low (10000X) and high (50000) magnification top-view SEM images of ZnO films obtained in -0.90 V

Figure 3e. Relatively low (10000X) and high (50000) magnification top-view SEM images of ZnO films obtained in -1.16 V

3.3. Optical Properties of the ZnO Films

The optical properties of the films were researched by using absorbance measurements at wavelength from 300 nm to 600 nm. The absorbance measurements versus wavelength of the films are demonstrated in Fig. 4.The films obtained at different cathodic potentials shown that have strong absorber features at under wavelength of 342nm. Fig 5 is indicated the transmittances of the ZnO films . It is clearly seen from the Fig. 5 that the ZnO films shows relatively low transmittance. The cause for this situation can be resulted from high surface roughness. The optical band gaps of the films for direct allowed transition were declared Tauc relation which is notified following equation

$$(\alpha h\nu)^2 = A(h\nu - Eg) \tag{12}$$

where A is a constant, hν is the photon energy, Eg is the band-gap, α is the absorption coefficient [12,13]. Fig. 6 is demonstrated the Tauc plots of the produced films The band gaps were computed to using graphical plot of $(\alpha h\nu)^2$ towards hν indicated in Fig 6. The extrapolation of the curves is obtained the energy axis which is indicated between 3.50 eV and 3.56 eV for ZnO films which are represented in Table 1. These band gaps values didn't devise any relationship intermediate to the band gaps and cathodic voltages.
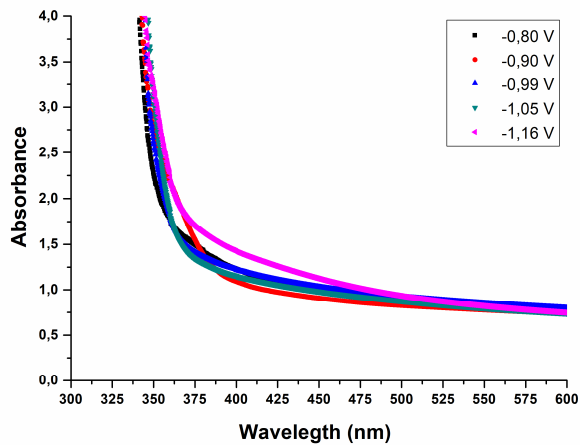

Figure 3c. Relatively low (10000X) and high (50000) magnification top-view SEM images of ZnO films obtained in -0.99 V

Figure 4. Optical absorption spectra of the ZnO films obtained in -0.80 V cathodic potential to -1.16 V, the wavelength range from 300 to 600 nm.
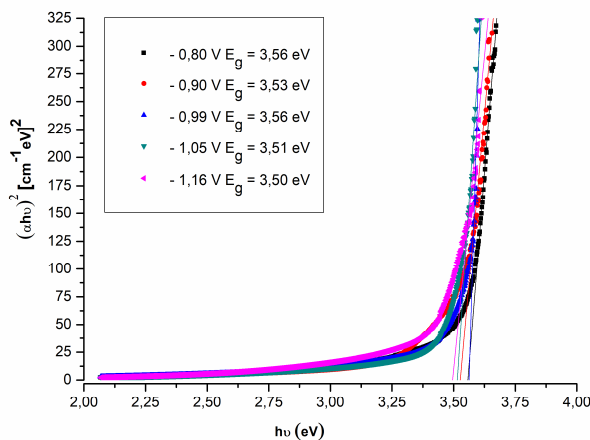

Figure 5. Plots of $(\alpha h\upsilon)^2$ vs. $h\upsilon$ for the ZnO films obtained in -0.80 V cathodic potential to -1.16 V
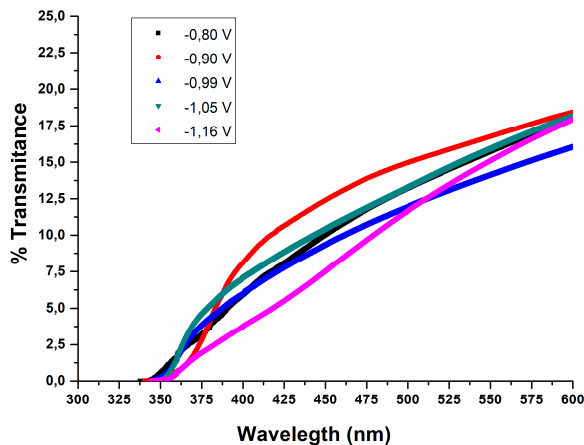

Figure 6. Optical transmitance spectra of the ZnO films obtained in -0.80 V cathodic potential to -1.16 V, the wavelength range from 300 to 600 nm.

4. CONCLUSION

In this work ZnO films were obtained by electrodeposition at different cathodic potentials ranging from -0.8 V to -1.16 V. The final solutions were saturated with oxygen during the depositions so rod-like structures weren't obtained. Because of the fact that ZnO widely uses gas sensor, it was important that ZnO didn't obtain rod-like structures. ZnO crystals were formed in slice-like structures. Therefore, surface roughnesses were increased and ZnO films were suitable for gas sensors. It was seen from the XRD pattern that as cathodic potentials increased, the peak intensities increased and XRD pattern revealed all films formed in hexagonal crystal structure. The bandgap of the films was estimated by using Tauc plot. The bandgap of the films varied between 3.50 and 3.56 eV.

REFERENCES

[1]   J. Wellings, N. Chaure, S. Heavens ve I. Dharmadasa, ''Growth and characterisation of electrodeposited ZnO thin films'', Thin Solid Films, vol.516, pp. 3893-3898, 2008.

[2]   D. A. Hamdane Chettah, ''Effect of the electrochemical technique on nanocrystalline ZnO electrodeposition, its'', Thin Solid Films. vol. 537, pp. 119-123, 2013.

[3]   Q. Wang, Q. Cao, X. Wang, B. Jing, H. Kuang and L. Zhou, ''A high-capacity carbon prepared from renewable chicken feather biopolymer for supercapacitors'', Journal of Power Sources, vol. 225, pp. 101-107, 2013.

[4]   A. Azizi, M. Khelladi, L. Mentar and V. Subramaniam, ''A study on Electrodeposited of Zinc Oxide Nanostructures'', Journel of Materials Science Materials in Electronics, vol. 24, no.1, pp. 153-159, 2013.

[5]   C. Lin, . H. Lin, J. Li and X. Li, '' Electrodeposition preparation of ZnO nanobelt array films and application to dye-sensitized solar cells'', Journal of Alloys and Compounds, vol. 462, pp. 175–180, 2008.

[6]   M. Va´zquez and M. Berruet, ''Electrodeposition of single and duplex layers of ZnO with different morphologies and electrical properties'', Materials Science in Semiconductor Processing, vol. 13, pp. 239-244, 2010.

[7]   J. A. R. Márquez ve C. M. B. Rodr, '' Effect of Surface Morphology of ZnO Electrodeposited on Photocatalytic Oxidation of Methylene Blue Dye Part I: Analytical Study'', Int. J. Electrochem. Sci., vol. 6, pp. 4059-4069, 2011.

[8]   R. Bhowmik, M. N. Murty and E. S. Srinadhu, ''Magnetic modulation in mechanical alloyed $Cr_{1.4}Fe_{0.6}O_3$'', PMC Physics B., pp. I : 20., 2008.

[9]   A. H. Mundher, ''Preparation and characterization ZnO nanoparticles and study of morphology at high

temperature'', Iraqi Journal of Physics, vol. 10, no. 18, pp. 17-23, 2012.

[10] M. Chaari, A. Matoussi and . Z. Fakhfakh, ''Structural and Dielectric Properties of Sintering Zinc Oxide Bulk Ceramic'', Materials Sciences and Application, vol. 2, pp. 765-770, 2011.

[11] T. Mahalingam, V. S. John and L. S. Hsu, '' Microstructural Analysis of Electrodeposited Zinc Oxide Thin Films'', Journal of New Materials for Electrochemical Systems, vol. 10, pp. 9-14, 2007.

[12] A. M. Palve and S. S. Garje, '' Preparation of Nanostructured Zinc Oxide from Single Source Precursors'', Synthesis and Reactivity in Inorganic, Metal-Organic, and Nano-Metal Chemistry, vol. 40, pp. 153–156, 2010.

[13] M. Yilmaz, D. Tatar, . E. Sonmez ve . C. Ci, ''Investigation of Structural, Morphological, Optical,and Electrical Properties of Al Doped ZnO Thin Films Via Spin Coating Technique'', Synthesis and Reactivity in Inorganic, Metal-Organic, and Nano-Metal Chemistry, vol. 46, pp. 489-494, 2016.